REPORT DOCUMENTATION PAGE	AFRL-SR-AR-TR-05-0294

Public reporting burden for this collection of information is estimated to average 1 hour per respo... instructions, searching existing data sources, gathering and maintaining the data needed, and com... information. Send comments regarding this burden estimate or any other aspect of this collection ..., including suggestions for reducing this burden to Department of Defense, Washington Headquarters Services, Directorate for Information Operations and Reports (0704-0188), 1215 Jefferson Davis Highway, Suite 1204, Arlington, VA 22202-4302. Respondents should be aware that notwithstanding any other provision of law, no person shall be subject to any penalty for failing to comply with a collection of information if it does not display a currently valid OMB control number. **PLEASE DO NOT RETURN YOUR FORM TO THE ABOVE ADDRESS.**

1. REPORT DATE *07/04/2005*	2. REPORT TYPE Final	3. DATES COVERED *(From - To)* 01/12/2001-30/11/2004

4. TITLE AND SUBTITLE
Development of Stress Gradient Enhanced Piezoelectric Actuator Composites

5a. CONTRACT NUMBER
F49620-02-1-0030

5b. GRANT NUMBER

5c. PROGRAM ELEMENT NUMBER

6. AUTHOR(S) Christopher S. Lynch

5d. PROJECT NUMBER

5e. TASK NUMBER

5f. WORK UNIT NUMBER

7. PERFORMING ORGANIZATION NAME(S) AND ADDRESS(ES)

AND ADDRESS(ES)
The GWW School of Mechanical Engineering, The Georgia Institute of Technology, Atlanta, GA 30332-0405

8. PERFORMING ORGANIZATION REPORT NUMBER

9. SPONSORING / MONITORING AGENCY NAME(S) AND ADDRESS(ES)

Dr. Byung-Lip Lee
AFOSR~~/NL~~ NA
801 N. Randolph St.

Arlington, VA 22203

10. SPONSOR/MONITOR'S ACRONYM(S)
AFOSR

11. SPONSOR/MONITOR'S REPORT NUMBER(S)

12. DISTRIBUTION / AVAILABILITY STATEMENT Approved for public release, ~~distribution unlimited~~

13. SUPPLEMENTARY NOTES

14. ABSTRACT
This report describes a multifunctional skin material that integrates piezoelectric layers to achieve multiple functions. These materials act as structural elements, have embedded piezoelectric actuation for shape control and active vibration suppression, and have in integral NDE system that utilizes a portion of the piezoelectric element for the detection of delaminations and cracks. Classical lamination theory modified to include piezoelectric layers was used as a design tool for the development of the skin material. The design utilized differential thermal expansion during processing to induce a residual compressive stress in the piezoelectric layer of the active skins resulting in high reliability and good resistance to fatigue.

15. SUBJECT TERMS

16. SECURITY CLASSIFICATION OF:			17. LIMITATION OF ABSTRACT	18. NUMBER OF PAGES	19a. NAME OF RESPONSIBLE PERSON
a. REPORT	b. ABSTRACT	c. THIS PAGE			19b. TELEPHONE NUMBER *(include area code)*

Standard Form 298 (Rev. 8-98) Prescribed by ANSI Std. Z39.18

7-21-05

20050722 054

Executive Summary

The following report describes the development of fiber epoxy laminates with integral piezoelectric layers. The laminates were designed to induce a compressive stress in the piezoelectric ceramic layer, thus eliminating cracking issues. When a voltage is applied to the piezoelectric layer, a change of curvature is induced in the laminate. This results in actuation capability. A significant portion of the effort focused on development of design tools for predicting the initial curvature, the change of curvature with voltage, and the residual stress state in the laminates; development of manufacturing techniques for reproducible production of actuators, and testing of the actuators for reliability. In addition to the actuation capability, the electrodes were patterned to isolate small segments of the piezoelectric layer for use as an integral ultrasonic damage monitoring system. One segment of the piezoelectric was used to launch an acoustic wave across the laminate. A second segment of the piezoelectric was used to receive this wave. If there was damage in the region between the source and receiver of the acoustic signal, it could be detected.

The results of this program are published in a series of journal and conference articles that are referenced herein. Significantly more detailed results are found in four Masters of Science Theses in the Georgia Tech library. These results are summarized in detail herein. In addition, the MATLAB code used to design the composites in included as an appendix.

Objectives

The objective was the development of stress gradient enhanced piezoelectric actuator composites which represent the next generation of a family of unimorph based curved actuators that obtain enhanced performance from the presence of a stress gradient in the piezoelectric material. This actuator family includes Rainbow and Thunder actuators. The development was to have represented a significant improvement to existing technology through control of the stress gradient within the piezoelectric layer. It turned out that the stress gradient in the piezoelectric material itself did not have the effect on actuator performance that had previously been speculated about, but control of the stress gradients in the composite was critical to obtaining excellent fatigue performance.

As with other unimorphic designs, these composites change their curvature in response to an applied voltage. Similar piezoelectric plate / fiber epoxy laminate devices had previously been demonstrated in other research laboratories, but adequate design tools were not available to predict their curvature, response to voltage, and the effects of stress gradients on the response.

The resulting actuators will be useful for multiple Air Force related applications. They are well suited for active vibration suppression. Development of the design tools has enabled manufacturing them with a controlled initial curvature that matches that of an aircraft skin. This will optimize their response in applications such as active control of twin tail buffet. Integral ultrasonic monitoring has been demonstrated to be suitable for evaluation of possible damage to the actuator and could potentially be used to monitor the health of the skins between the actuators. Strategically placed actuators could be used to triangulate the position of delaminations or to monitor the evolution of distributed damage of individual actuators and in regions between them.

Results include the development, laboratory scale production, and testing of piezocomposite actuators. Design tools were developed based on composite laminate theory and non-linear and hysteretic piezoelectric constitutive behavior. The integral ultrasonic damage detection system was evaluated and results correlated with the introduction of controlled flaws.

Specific research objectives stated in the initial proposal were to:

1. Develop bending mode stress gradient enhanced piezoelectric actuator composites (GEPACs). Such actuators make use of differential thermal expansion to control initial prestress and curvature. (Accomplished)

2. Develop and apply finite element design tools for prediction and optimization of stress gradient performance enhancement. This includes use of a Georgia Tech developed finite element code for analysis of the hysteretic behavior of ferroelectric ceramic materials associated with non-180° domain wall motion. The finite element code utilizes micromechanics based constitutive models. (Accomplished but not entirely successful.)

3. Explore the range of possible actuation modes. Different modes of actuation are be possible through control of the anisotropy of the fiber composite. Examples include utilization of twist coupling. Again the key factor that differentiates this approach from prior work on lamination of PZT plates into fiber reinforced composites is the use of differential thermal expansion to control the pre-stress state and thus enhance the piezoelectric response. (Accomplished)

4. Manufacture and test a series of actuators for function (low cycle testing). Measure blocked force and free displacement. Measure curvature and curvature change with applied electric field. Compare results with finite element code predictions. Most of the composite behavior can be predicted with available design tools. Research focus was on the actuator material including thickness effects and composition effects. (Accomplished)

5. Perform fatigue performance characterization. This included cycling with free displacement, with blocked displacement, and with an impedance matched load. High cycle degradation was investigated. (Accomplished)

6. Manufacture actuators with segmented electrodes. Part of the actuator performd as an ultrasonic transmitter and part as a receiver. This resulted in an integral damage detection system. The amplitude was sufficiently low and the frequency sufficiently high that the damage detection function did not interact with the primary function of the actuator. (Accomplished)

7. Perform independent evaluation of damage by ultrasonic C-scan and X-ray radiography. Correlate these results with those by the integral damage

detection/assessment system. (Altered. Co-PI changed institutions. Alternative approach was utilized.)

8. Perform fracture and damage mechanics analyses as part of the assessment of fatigue degradation such as possible delaminations at various locations within the composite, and distributed damage such as possible microcracking on the tensile surface of the PZT and within the composite. Propose design changes that will enhance performance and actuator life. Implement design changes in next generation of actuators. (Accomplished)

Personnel Supported

C.S. Lynch	Faculty	P.I.	Partial Summer salary support
Y. Berthelot	Faculty	Co-P.I.	Partial Summer salary support
K. Weber	M.S. Ph.D.	Ferroelectric Composite Actuator Design, Fabrication, and Evaluation	M.S. Spring 2005 Expected Ph.D. Spring 2007
D. Hopkinson	M.S.	Development of Stress Gradient Enhanced Composite Unimorph Actuators	M.S. Spring 2003
A. Bechet	M.S.	Ultrasonic Detection of Debonding within a Gradient Enhanced Composite Actuator	M.S. Spring 2003
D. Gex	M.S.	Ultrasonic NDE testing of a Gradient Enhanced Piezoelectric Actuator (GEPAC) undergoing low frequency bending excitation	M.S. Spring 2004

Publications

Refereed Journal Articles

A. Bechet and Y. Berthelot, C.S. Lynch, "A Stress Gradient Enhanced Piezoelectric Actuator Composite (GEPAC) with Integrated Ultrasonic NDE Capability for Continuous Health Monitoring," Accepted for Publication, *Journal of Intelligent Materials Systems and Structures (JIMSS-03-065) (2004)*

K. Weber, D. Hopkinson, C.S. Lynch, "Development of Unimorph Piezoelectric Composite Actuators", Accepted for publication in *Journal of Intelligent Materials Systems and Structures*

D. Gex, Y.H. Berthelot, C.S. Lynch, " Low frequency bending piezoelectric actuator with integrated ultrasonic NDE functionality," to appear in Int. J. Nondestructive Eval., 2005

Conference Proceedings

D. Hopkinson and C.S. Lynch, "*Design of Small and Large Scale Piezoelectric Unimorph Composites*" Proceedings of the American Society for Composites 18th Technical Conference

D. Hopkinson and C. S. Lynch, "Design of Single Crystal Piezoelectric Composite Unimorph Actuators" Proceedings of IMECE 2003, ASME International Mechanical Engineering Congress and Exposition, Applied Mechanics, Constitutive Relations of Advanced Materials, Washington, D.C., USA, November 16-21, 2003

Theses

Four M.S. Theses were written and are available through the Georgia Tech Library. Summaries of key findings follow.

DEVELOPMENT OF STRESS GRADIENT ENHANCED PIEZOELECTRIC COMPOSITE UNIMORPH ACTUATORS

A Thesis

Presented to

The Academic Faculty

By

David P. Hopkinson

July, 2003

Executive summary

The purpose of this study was to develop manufacturing techniques to produce reliable piezoelectric unimorph actuators made from composite materials, as well as to characterize and model them. Piezoelectricity is a property of certain crystalline materials that causes them to produce an electric voltage when they are deformed by an applied stress, and conversely causes them to elongate or contract when an electric field is applied to them. A unimorph actuator in its simplest form consists of a piezoelectric plate that is bonded to a non-piezoelectric plate. When an electric field is applied to the actuator, the piezoelectric plate expands or contracts and the non-piezoelectric plate resists this motion, causing the actuator to displace in a bending motion.

Although there are many potential applications for this technology, one particular application of interest is to control vibrations in an aircraft, such as twin tail buffet. At high angles of attack, air flow vortices form due to flow separation at the leading edges of the wings. These vortices can cause large amplitude vibrations in the tails of aircraft with two vertical stabilizers. This phenomenon could be alleviated by embedding unimorph composite actuators into a multifunctional aircraft skin for active vibration suppression. Other areas of use for piezoelectric bending actuators include loud speakers, pressure sensing, noise control, and precision position controlling.

These composite actuators are fundamentally similar to previous generations of unimorph actuators such as Thunder, which consists of a lead zirconate titanate (PZT) ceramic plate laminated to a stainless steel substrate. The laminate is bonded at a high temperature, and upon cooling it forms an initial curvature due to differential thermal expansion of the two materials. A residual stress gradient occurs in the piezoelectric material causing enhanced flexural strains in the actuator. Composite actuators apply these same principles, but consist of a piezoelectric material bonded between two or more layers of fiber reinforced polymer composite materials. Using composite layers instead of metal layers allows for greater control of the actuator characteristics using the anisotropic properties of the composite materials. Other advantages include reduced weight, and better integration into a composite aircraft skin.

A review of other research that is relevant to this study is discussed in Chapter 2. This includes the design and modeling of traditional metal unimorph actuators as well as composite unimorph actuators. Fundamental piezoelectric theory is also reviewed.

The design of the actuators and the development of manufacturing techniques has been an evolutionary process, which is discussed in Chapter 3. An autoclave was used to control the cure cycle of the composite layers. The actuators were vacuum bagged and cured inside of the heated and pressurized autoclave chamber. They cannot be cured in a hard die like a standard composite panel, because it causes cracking of the fragile PZT ceramic. Piezoelectric materials are also temperature sensitive, and can lose their piezoelectric properties if heated above a certain temperature.

Experimental results are discussed in Chapter 4. The actuators are characterized according to their displacement and force output. Displacement was measured using a linear variable differential transducer (LVDT) at various force loads. Strain was measured on the top and the bottom of the actuators using strain gauges, which can be used to calculate curvature and displacement. The displacement that was calculated from the strain gage data is independent of the LVDT, and was used to verify the measurement. The force was adjusted by loading the top of the actuator with weights. For piezoelectric actuators, there is always a trade-off between force and displacement. An actuator that can produce a higher displacement will generally produce less force, and vice-versa.

The composite actuators were modeled using classical lamination theory, which is also discussed in Chapter 4. Classical lamination theory is well suited for predicting the stress distribution, strain distribution, and curvature of anisotropic materials that are bonded together in a multi-layered laminate. It is important to know the stress distribution in the laminate so that the piezoelectric layer can be designed to stay in residual compression. Since the piezoelectric material is very brittle, this can prevent cracking. Calculating the strain distribution is useful for locating the neutral axis of the laminate, which occurs where the strain is equal to zero. The two primary forces that act on the actuator are thermal expansion and expansion of the piezoelectric layer. The model is used to calculate the initial curvature caused by thermal expansion, and the change in curvature caused by piezoelectric coupling. For simplicity, this model assumes that the piezoelectric material operates in a linear regime, but in reality the piezoelectric material exhibits some non-linearity and hysteresis, largely due to domain wall motion. A computer program has been written using Matlab that allows a user to input the parameters of a composite actuator and quickly find out the stress distribution, strain distribution, and curvature. The code is included as Appendix A.

Two innovative types of composite actuators were manufactured and compared to conventional composite actuators. The first had a brickwork array of PZT plates, rather than one large PZT plate. This design is useful for making large surface area actuators, since it is impractical to manufacture a very large actuator with a single PZT plate. The other non-conventional actuator was designed with a single crystal piezoelectric plate. Single crystals can produce up to five times the strain of a comparable polycrystalline piezoelectric material, but they have a lower Young's modulus, are difficult to grow into large sizes, and are generally more expensive.

Chapter 5 summarizes the accomplishments of this study. Conclusions from the experimental and model results are discussed, and recommendations for future extensions of this research are made.

Key Results

This work successfully advanced the development of a relatively new class of piezoelectric unimorph actuators that are made from composite materials. These

actuators were made from a layer of PZT ceramic material that was bonded between electrically insulating layers of unidirectional Kevlar / epoxy prepreg. The Kevlar layers were oriented at 90° on the bottom of the PZT and at 0° on top of the PZT. After curing in an autoclave, the actuators became curved and pre-stressed due to differential thermal expansion of the different orientations of Kevlar. The curvature could be controlled in response to an electric field due to piezoelectric coupling.

One of the key features of these actuators was the stress gradient that was induced in the actuators after curing. This stress can cause ferroelastic domain wall motion in the piezoelectric material. When an electric field is applied, it will cause the domains to align in the direction of the field. This domain wall motion causes the piezoelectric material to exhibit an enhanced strain response, greater than the response from expansion and contraction of the unit cell alone.

The actuators were characterized using an LVDT to measure displacement, and strain gages that were used independently to verify the displacement measurements from the LVDT. The displacements that were calculated from the strain data were consistent with the LVDT measurements. Several identical specimens were manufactured to test the consistency of the results, and they were found to have good repeatability.

A linear model was developed for the composite actuators using classical lamination theory. The model predicts the curvature, stress distribution, and strain distribution of a laminate by integrating the stress contributions of each layer to find forces and moments. The primary sources of stress within the laminate are due to thermal and piezoelectric expansion. The model proved to be a useful design tool for ensuring that the piezoelectric layer remains in residual compression, for locating the neutral axis, and for optimizing the initial curvature due to thermal expansion and the change in curvature due to piezoelectric coupling.

Because the ultimate goal of these actuators is to actively control the shape of a large surface, it was necessary to design an actuator that makes use of an array of piezoelectric plates rather than a single plate. It would be impractical to use a single piezoelectric plate in a very large actuator, and therefore a brickwork type actuator was developed. The brickwork actuator was successful in that it could be manufactured on either a small or a large scale, and the resulting curvature response was predictable and

proportional regardless of size. However, a brickwork actuator produced displacements that were only about 50% of an equivalent actuator made from a single piezoelectric plate. This was expected, though, because the gaps between piezoelectric plates in a brickwork actuator cause additional edge effects and absorb some of the piezoelectric strain.

Another variation of the composite unimorph design that was tested had a PZN-4.5%PT single crystal piezoelectric plate instead of a PZT polycrystalline ceramic. The single crystal material has a d_{311} strain coefficient that is five times higher than the ceramic, and was therefore expected to produce a large displacement response when integrated into a unimorph actuator. Experimentally, the PZN-4.5%PT actuator had a very similar response to electric field as the PZT actuators. PZN-4.5%PT has a much smaller stiffness than PZT, which severely limited the ability of the single crystal material to deform the relatively stiff Kevlar substrate. Also, the residual compressive stress may have caused a phase transformation in the PZN-4.5%PT that reduced its piezoelectric properties. PZN-4.5%PT may still be useful for unimorph applications, but will require a different actuator design, rather than being used as a direct substitution for PZT.

ULTRASONIC DETECTION OF DEBONDING WITHIN A GRADIENT ENHANCED PIEZOELECTRIC ACTUATOR (GEPAC)

A Thesis

Presented to

The Academic Faculty

By

Antoine Béchet

Georgia Institute of Technology

June, 2003

Executive summary

The purpose of this work was to set up a non destructive evaluation method to detect debonding defects intrinsic to the actuators. Gradient Enhanced Piezoelectric Actuators, or GEPAC's, are very thin piezoelectric plates embedded between two layers with different thermal expansion properties. These actuators provide superior performance for operations at low frequencies as compared to traditional actuators and they should find some useful applications in the aeronautical industry in particular, for instance, in the development of "smart skins". GEPACs represent the next generation of a family of unimorph based curved actuators that produce enhanced performance from the presence of a stress gradient in the piezoelectric material. As with other unimorph designs, GEPACs change their curvature in response to an applied voltage.

GEPACs will be useful for multiple Air Force related applications. On one hand they are well suited for active control of vibration, in the low frequency range. They can be manufactured to match the curvature of the aircraft skin. On the other hand these actuators can also be used for ultrasonic nondestructive evaluation. Indeed, the design allows the actuators to detect damage to itself, debonding between the actuator and the

aircraft skin in which they are embedded, as well as delaminations in the material between an array of actuators (see Figure 1.1).

Manufacturing the actuators with segmented electrodes enables one end to act as an ultrasonic transmitter and the other to act as the receiver. When a pulsed voltage is applied to the transmitting electrode, by virtue of the piezoelectric effect, an acoustic pulse is launched through the piezoelectric plate, and it is received on the other side (see Figure 1.2). Again, because of the piezoelectric effect, the received ultrasonic pulse is converted into an electrical pulse. The traveling pulse is affected by the surface boundary conditions, i.e., by the bound quality between the piezoelectric plate in the outer plates. In this configuration, the existence of a debonding defect should be detectable. The attractive feature of this inspection technique is that the actuator is imbedded in the skin of the aircraft, and that the amplitude of the ultrasonic wave is sufficiently low and the frequency sufficiently high that the damage detection function should not interact with the primary function of the actuator (low frequency, high amplitude).

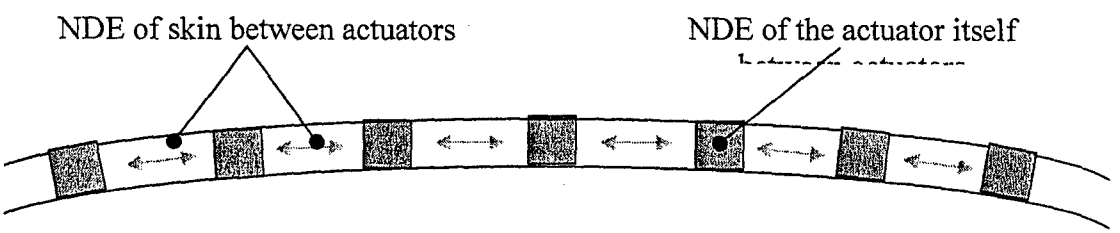

Figure 1.1 – Actuators embedded in an aircraft wing.

The work presented in this thesis has been conducted on a single configuration of flat actuators. The actuator studied is composed of a flat piezoelectric layer (TRS600, 25 mm x 10 mm x 0.5 mm) glued to a top steel layer (40 mm x 10 mm x 0.126 mm) and to a

bottom steel layer of same dimensions, containing a simulated defect, as shown in Figure 1.2. For simplicity, the debonding defect is simulated by a rectangular cut done on the bottom steel layer through its entire width. It is also assumed that the initial bending curvature of GEPACs is negligible in comparison to the wavelength of the ultrasonic wave (at 1MHz, $\lambda = 5\ mm$).

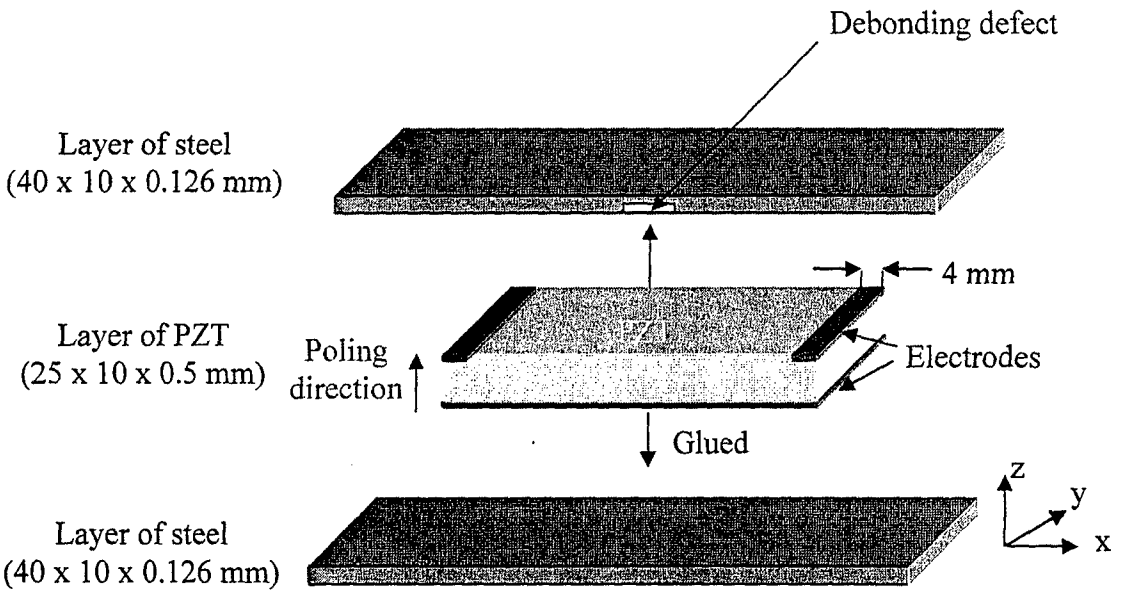

Figure 1.2 – Flat Actuators Steel-PZT-Steel.

The thesis is organized as follows. Chapter 2 provides the necessary background on piezoelectricity, waveguide dispersion, and analytical computations of the slowness and dispersion curves for a piezoelectric plate. Chapter 3 is devoted to the Finite Element Method. The FEM is a powerful method to simulate ultrasonic pulse wave propagation in solids. An important goal of the research was to develop such a numerical tool because of its wide range of applicability, and its ability to model and gain physical insight into ultrasonic propagation in plates and other complex geometries. With his numerical tool, a parametric study of the effect of the defect size (length and depth) on the measured

ultrasonic pulse has been conducted in order to characterize quantitatively the debonding defect. The results of the experimentation achieved on actuators are discussed in Chapter 4. A comparison between experimental and numerical results will be considered at the end of Chapter 4 to validate the Finite Element Model. In the Chapter 5 the future directions of the research are presented and related issues explored. Conclusions and recommendations are summarized in the last chapter.

Key Results

In this thesis, it was established that, by segmenting the electrodes of the PZT actuator, one can generate and receive an ultrasonic pulse within the actuator itself. The ultrasonic pulse that propagates within the actuator is affected by a defect in boundary condition (such as a delamination between the PZT and the outer skin). In other words, the integrity of the actuator itself can be monitored in real-time, continuously, using this ultrasonic NDE approach.

The actuator studied was composed of a flat piezoelectric layer (TRS600, 25 mm x 10 mm x 0.5 mm) glued to a top steel layer (40 mm x 10 mm x 0.126 mm) and to a bottom steel layer of same dimensions, containing a simulated defect. The range of defect went from 0 mm up to 12.5 mm in length. Defects were machined in the lower plate by removing a thin layer of steel in order to simulate debonding between the PZT and the outer layer. While very crude, this known defect is nevertheless a simple way to assess the feasibility of the ultrasonic NDE technique for this application. It was found that such defect in the boundary between the plate and the outer layer can be detected by monitoring the propagation of one cycle of a 1 MHz pulse sine wave, symmetric (compressional) pulse. This frequency is a good compromise between detecting small defects, which requires high frequencies, and propagating a non-dispersive signal, which is much simpler to analyze.

Both experiments and numerical modeling showed that the proposed NDE technique is suitable to detect defects. The numerical analysis was based on the Finite Element Model (FEM) code ABAQUS explicit, which is well suited to model pulse propagation at ultrasonic frequencies in a plate. The FEM code was developed for the flat actuators used

in the experiment, for both two and three-dimensional geometries. Experiments and models showed that the initial part of the received signal contains all the useful information about the possible presence of a defect. The later part of the received signal is much more difficult to analyze because it contains a superposition of many reflections throughout the sample. Also, a useful result is that the initial part of the signal is predicted to be the same whether one uses the 2D model or the 3D model. A correlation technique was developed as an effective way to detect and quantify the defect. First, the signals were gated to eliminate the late arrivals and the complications associated with these late reflections. Then, the signal was correlated with a reference signal, (signal obtained without defect). In a real-time implementation, the reference signal would be the signal within the actuator during early operations, well before failure might occur. Both numerical (FEM) computations on a PC and experiments showed good agreement in the early part of the time domain signal, and both showed that the correlation technique is a robust method to detect the presence of a defect.

Looking at further applications, a preliminary experiment was carried out in a large plate (12 inches by 16 inches) made of two plies of fiberglass, in which two small PZT actuators were embedded and separated by 4 inches. In this case the PZT actuators were not segmented. The objective was to use the first PZT plate as the source and the second as the receiver to detect a possible defect between the two PZT transducers. The received signal showed very large signal-to-noise ratio, and extremely simple signal to analyze, because reflections from the edges of the plate were not superimposed on the direct arrivals. This technique is very promising for detection of defects between embedded actuators over very large distances, up to a foot or more. Future work along these lines could concentrate on the detection of delamination damages in the material between an array of actuators. The experience acquired from this work will be useful to implement quickly both experimental and numerical computation analysis. The Finite Element Model for this problem of long range propagation in the plate actually appears to be numerically less demanding than the one performed in this thesis. Finally, a logical next step would be to demonstrate the ultrasonic NDE capability superposed on the low frequency actuation of a GEPAC actuator.

Ultrasonic NDE testing of a Gradient Enhanced
Piezoelectric Actuator (GEPAC) undergoing low frequency bending excitation

A Thesis
Presented to
The Academic Faculty

By

Dominique Gex
Georgia Institute of Technology
April 2004

Executive Summary

Gradient Enhanced Piezoelectric Actuators, or GEPACs, consist of very thin piezoelectric plates embedded between several composite layers with different thermal expansion coefficients. The actuators are designed to place the active ceramic layer in residual compression. Compared to traditional actuators, GEPACs provide superior performance in the bending mode for operations at low frequencies. They can be of high interest in aeronautics for the construction of "multifunctional skins". As with other unimorph designs, GEPACs change their curvature in response to an applied voltage. One could therefore actively control the shape of an airfoil to improve aerodynamic performance or actively damp vibration. Bending mode actuators that produce large deflections have been developed such as the rainbow and the Thunder actuators. These devices are based on using residual stresses to improve the piezoelectric response of the actuator. They use stainless steel or other metal as a substrate to the PZT plate. Goo recognized the benefit of using fiber composites instead of metal. Lynch et al. built such

actuators and finite element models and called them GEPAC. While GEPACs have great potential for a variety of applications, they may be susceptible to fatigue-induced damage. Delamination or debonding may occur between the PZT layer and the fiber composites, cracks in the thin PZT layer may also be present either after manufacturing of the actuator, or possibly, after millions of cycles of use (fatigue).

The objective of the present research is to show that ultrasonic Non Destructive Evaluation (NDE) can be used to monitor the structural integrity of the actuator itself while it is performing its low frequency bending actuation. Preliminary work by Bechet included a finite element model of ultrasound in a GEPAC actuator, using Abaqus/explicit, and proof-of-concept experiments. For simplicity of modeling and experimentation, Bechet modeled a PZT plate sandwiched between two steel plates. In a GEPAC actuator, the PZT plate is sandwiched between several layers of fiber composite materials. The experimental results reported in this thesis demonstrate that ultrasonic NDE can be used in a GEPAC actuator to monitor its structural intergrity while not interfering with the primary function of the actuator in the low frequency bending mode.

The thesis is organized as follows. Chapter 2 provides some background information on currently available bending actuators, as well as the design and manufacturing of GEPAC actuators in our laboratory at Georgia Tech. Chapter 3 is devoted to operations of ultrasonic non destructive evaluation and low frequency actuation in a GEPAC. The focus is on the propagation of acoustic wave in the actuator and observation of the effect of actuation on the ultrasonic NDE function. Chapter 4 addresses the results of fatigue testing of a GEPAC. Fatigue experiments were conducted (up to 53 millions cycles of actuation) and the actuator regularly inspected by ultrasonic NDE in order to evaluate possibly degradation. Fatigue testing was performed on healthy actuators and debonding defects were studied. Chapter 5 presents experimental results obtained with a fiber-composite plate containing two thin embedded piezo ceramics separated by a distance of 180 mm. This experimental work was part of the development of the NDE capability to monitor the structural health of an actuator, and also to monitor structural health of a composite plate between two actuators over large distances. Experiments are reported for both healthy composite plates and for plates containing artificially induced debonding defects. Finally, conclusions and a summary are presented in the last chapter.

Key Results

Gradient Enhanced Piezoelectric Actuators, or GEPACs, are very thin piezoelectric plates embedded between several composite layers with different thermal properties. The anisotropic properties of the composite, and particularly the coefficient of thermal expansion leads to residual stresses that improves the actuator performance for low frequency actuation under high voltage (up to 500 V). These types of actuators are used primarily in the bending mode. Possible applications include "smart" active wings where the shape can be attered to improve performance. These actuators could also be embedded in an aircraft fuselage to provide means of actively controlling vibrations and interior noise. Because of the very thin (250 to 500 μm) piezoactive elements, it is important to be able to monitor the structural health integrity of these actuators while they are under low frequency actuation. The primary objective of this thesis was to establish that, by segmenting the electrodes of the actuator, one can perform ultrasonic nondestructive evaluation (NDE) of the actuator to detect the presence of cracks or debonding.

GEPAC actuators have been manufactured with multiple layers of unidirectional Kevlar fiber epoxy (0° / 0° / 90° / PZT / 90° / 90°) and cured in an autoclave at 177°C at 30 psi. The top electrode of the PZT was segmented by gently rubbing sandpaper. In all the results presented in this thesis, the input voltage for the ultrasonic signal was one cycle of a 1 MHz sine wave with amplitude of 5 V. At this frequency, the wavelenght is much longer than the thickness of the PZT. Nevertheless, because of the multi layered structure and the anisotropy of each layers, the received ultrasonic signal is rather complicated.

Experiments showed that the repeatibility of the signal was excellent, not only for the early arrivals but also for the very late arrivals, which correspond to the "reverberation" of ultrasound in the sample. Despite the complexity of the signal, the reverberation signature for a given GEPAC is very repeatable. It was also established that utrasonic signals can be used to detect cracks in the actuator if the crack occurs after curing. If it

occurs during manufacturing, resin fills up the crack and ultrasonic signals are not significantly affected by the presence of resin filled cracks.

In this thesis, it was also established that the low –frequency, high voltage, high amplitude actuation of the device does not interfere with the high-frequency, low voltage, low amplitude of ultrasonic signals. It is therefore possible to monitor the structural integrity of the GEPAC actuator in real time while it undergoes low frequency actuation.

Fatigue testing of the GEPAC actuators was studied by measuring ultrasonic signals during life cycle up to 53 million cycles. No visible signs of fatigue could be observed up to 24 million cycles. Even late arrivals (ultrasonic reverberation) was remarkably similar for N=0 and N=24 $\times$ 10_6 cycles. After 27 million cycles, the main early part of the ultrasonic signal remained unchanged, but the late arrivals were noticeably different for N=0 and N=27 $\times$ 10_6 cycles. These experiments suggest that changes in the late arrivals (ultrasonic reverberation of the sample) are more sensitive to early signs of fatigue than the main ultrasonic signal. This result may be very useful for practical implementation of structural health monitoring of GEPAC actuators with ultrasound NDE. Interestingly when the fatigue test was continued up to 53 $\times$ 10_6 cycles, no changes could be detected for either the early or the late arrivals. Finally, experiments were conducted with two GEPAC actuators embedded in a Kevlar/epoxy plate, and separated by a distance of 180 mm. It was observed that (a) ultrasound (1 MHz pulse) propagates over this distance with enough amplitude that it can be used for NDE; (b) there is a noticeable difference between the ultrasonic signals in a healthy and a damaged composite plate. To artificially create debonding between the layers of the Kevlar epoxy plate, a release film was introduced during the manufacturing between two layers and removed after curing. A simple method to assess the presence of a defect is to measure the rms-signal amplitude of the received pulse. This method, however, does not allow one to localize the defect. GEPAC with segmented electrodes are therefore promising for ultrasonic NDE monitoring of structural integrity of actuators and skins in aeronautical applications. Future work could include the problem of large arrays of embedded GEPAC actuators for large scale applications.

Ferroelectric Composite Actuator Design, Fabrication, and Evaluation

A Thesis

Presented to

The Academic Faculty

By

Kyle G. Weber

Georgia Institute of Technology

Executive Summary

ECLIPSE actuators consist of a PZT ceramic plate sandwiched between layers of a unidirectional Kevlar 49/epoxy composite. Unidirectional Kevlar composite used during this study has anisotropic characteristics. The coefficients of thermal expansion parallel and perpendicular to the fibers are different. Curvature in a composite structure will form when the fibers of one layer are oriented perpendicular to the fibers of another in an unsymmetric layup. If a PZT plate is placed in between the Kevlar plies prior to curing, the entire structure will curve and a beneficial compressive stress will be induced through the brittle PZT. The stress allows the actuator to obtain large displacements without the piezoelectric material cracking. When an electric field is applied to the piezoelectric plate it reacts by expanding or contracting. This reaction is resisted by the composite material which causes a change in the actuator radius of curvature and a visible displacement. If the movement of the actuator is restricted, then a force is produced. This study focuses on actuator manufacturing, characterization of high and low cycle reliability, and actuator force output.

There are many potential applications for ECLIPSE actuators. Because an ECLIPSE actuator is curved, it would fit seamlessly onto a cylindrical structure. These actuators have a very low profile, have lower weight then other actuators made with metal, and can be bonded to the surface of a cylinder easily. Furthermore, these actuators could be readily integrated in to a composite structure, as the actuator is itself a composite. Composites are becoming more common in engineered structures; a composite based piezoelectric actuator, which could act as a sensor or receiver, would integrate well with these structures. Additional applications include control of low-frequency noise in passenger aircraft cabins (Simpson 1991), torpedo feedback sensors (Sumali 1991), unwanted vibrations in piping systems (White 1972), and submarine hulls (Clark 1993); all of which can be modeled as a cylinder.

ECLIPSE actuators are similar in operation to earlier generations of unimorph actuators, such as THUNDER and RAINBOW. Thin unimorph-like driver (THUNDER) actuators are made from a PZT plate bonded to a stainless steel substrate with LaRC-SI™ polyimide adhesive. The actuator is then cured in an autoclave at a high temperature. Upon removal from the autoclave a curvature and stress gradient are induced in the actuator due to the differences in thermal expansion between the piezoelectric material and stainless steel. Reduced and internally biased oxide wafer (RAINBOW) actuators are fabricated by chemically reducing a PZT plate into a substrate material at a high temperature. Upon cooling the differences in the coefficients of thermal expansion between the piezoelectric material and the substrate cause a curvature and stress gradient. In both the THUNDER and RAINBOW actuators, repoling is necessary after the curing process is completed due to the high curing temperature. ECLIPSE actuators are created using similar concepts, but a different manufacturing process is applied. ECLIPSE actuators are created by cutting and laying up composite plies with a PZT plate located between two layers. The entire stack is cured in an autoclave at a relatively low temperature. Repoling is not necessary after curing is completed due to the low curing temperature of Kevlar/epoxy composite. In addition, composite materials afford greater control over actuator characteristics. By changing the lay-up order, individual layer orientation, or composite material, the composite actuators can be tailored for specific applications.

A study of previous research on unimorph actuators similar to ECLIPSE actuators is reviewed in Chapter 2. A further review of other unimorph bending actuators is discussed along with a discussion of a class of actuators with two PZT plates called bimorph actuators. The fundamental constitutive relations of piezoelectric theory are also reviewed along with the important characteristics and behaviors of piezoelectric material such as poling, switching, and domain wall motion.

The manufacturing of ECLIPSE actuators is discussed in Chapter 3. The actuator materials are discussed individually along with the orientation of these materials in the final actuator product. The advantages and disadvantages of the chosen composite material are discussed in further detail. A miniature autoclave (MAC) was designed and built to make actuators in the convenience of the lab. MAC allows actuators to be built on a small scale reducing cost over the larger scale autoclave. The mold preparation, curing cycle process, and the post curing process are all discussed.

Due to out-of-plane deflections which are much greater then the thickness, modeling ECLIPSE actuators is difficult. Two models are presented in Chapter 4. The first model uses classical lamination theory to predict actuator behavior. Although this model is a good approximation, it is still a linear theory which cannot model non-linear behavior found in ECLIPSE actuators. The second model presented is the extended classical lamination theory which was developed at Virginia Tech by Michael Hyer. This model uses approximate displacement expressions which contain unknown coefficients. These coefficients are solved for by a series of substitutions and the minimization of a potential energy function. This technique contains non-linear terms in the strain relationships which help to account for non-linear actuator behavior. Both models were used to find the stress and strain distribution throughout the thickness of the actuators. This was done to ensure that the brittle piezoelectric plate remained in compression to prevent cracking. The strain distribution was also used to determine the neutral axis of the actuator. Neither the CLT nor ECLT models, which were used to predict the response of the actuators to an electric field, considered the hysteresis of the piezoelectric material, which is due largely to domain wall motion.

The experimentation and characterization results are seen in Chapter 5. ECLIPSE actuators were characterized by measuring the change in dome height of the actuator with a linear variable differential transducer (LVDT). The dome height of the actuators is related geometrically to the radius of curvature which can be calculated in CLT and ECLT. The change in dome height with change in electric field was studied for each different actuator layup and compared to both laminate theory models. The effect of moisture absorption by the composite material on the dome height displacement was also investigated. Additionally the cure temperature sensitivity of the models was tested and compared to measured values of actuators cured at various temperatures ranging from 157°C to 197°C. Fatigue testing was performed on the actuators to determine the useful service life. The resonant frequency was measured using a laser doppler vibrometer (LDV). Actuator specimens were cycled in an electric field range of 0 MV/m to 2 MV/m at resonance while a different set of actuators was tested at one half the measured resonant frequency with the same electric field range. All actuators tested were cycled unconstrained in a cantilevered setup. Cycling was stopped periodically to measure the displacement capabilities of the actuator to determine a decrease in performance. Finally, force output was measured using a four point bending apparatus and compared to the calculated values found in CLT and ECLT.

Chapter 6 discusses the conclusions of the experimental and modeling results. Recommendations are also made for future research.

Key Results

This work successfully progressed the understanding of unimorph composite actuator behavior under various conditions. Actuator design was improved over previous generations by eliminating extraneous composite material. This reduced the overall weight of the actuator and brought the measured actuator curvatures closer to those predicted. In addition, a miniature-autoclave was created that has the capability to produce multiple actuators daily without the expense of a full scale autoclave. This allowed actuators to be built locally, prepared, and tested daily.

An alternative model to the classical lamination theory model previously presented was introduced to predict actuator behavior. The extended classical lamination theory model began to explain the non-linear behavior of unimorph actuators due to large out of plane deflections. Both models presented were used to design actuators with the PZT material in residual compression. The curvatures were also calculated and compared to the displacements measured by the LVDT. The CLT model agreed well with the initial actuator curvature and reasonably predicted the displacement. The ECLT model under-predicted the initial curvature but correctly predicted the displacement trends.

The understanding of actuator behavior was further advanced by characterization of actuator behavior under various conditions. The actuators tested in this study were made from a Kevlar 49/epoxy composite. This composite material has limitations which include moisture absorption and UV sensitivity. Actuators were allowed to remain in a dark environment with access to atmospheric air to determine their performance with absorbed moisture. The actuators showed that there was no decrease in performance with small amounts of moisture absorbed into the composite. The sensitivity of Kevlar was also tested by curing actuators at various temperatures. It was shown that for the composite material used, no additional curvature can be obtained by curing the composite at a temperature above the manufacturer's recommendation. CTS 3195HD was the PZT material used in the actuators. Actuators were tested to determine their failure point. It was shown that while there was no definitive failure point, the actuators could be driven to a voltage higher then the recommended maximum voltage without the PZT material failing. Further, the actuator was shown to react linearly throughout the entire range of applied voltages without the piezoelectric effect saturating.

By restricting the displacement of these actuators a force will be produced. The force output of the actuators was measured by using a four-point bending apparatus. Various layups were tested to determine what the force capabilities were and whether there is a difference in force output between layups. It was found that the actuators with a PZT layer in a higher residual compressive state created more force.

The fatigue behavior of these devices was also examined. Two different loading conditions were considered. The first loading condition allowed one end of the actuator to move freely while the other was clamped. The resonant frequency of the actuator was measured with a LVDT. One set of specimens was cycled at the measured resonant frequency while another set was cycled at one half the measured resonant frequency. It was shown that the there was no decrease in displacement or shape of the minor hysteresis loop after a high number of cycles for either tested frequency. The second loading condition measured the force output of the actuator after a high number of cycles. It was shown that there was no decrease in actuator force capabilities due to cycling as well. These results strongly suggest that there were no interlaminate debonding, cracking the matrix, or cracking of the PZT material.

Additional work is required to further advance unimorph composite actuators. Other composite materials should be investigated to further refine the actuators performance. Kevlar 49 fiber has drawbacks that can limit the performance of the actuators. By selecting other materials without these shortcomings the actuators could perform better. Additionally, determining more accurate displacement approximations for the ECLT model would prove useful to modeling. Because these actuators could be useful to control the vibrations in a large cylindrical body, further investigation into the moment and force output would be necessary.

Appendix

MODIFIED CLASSICAL LAMINATION THEORY

MCLT requires several fundamental assumptions. The development of MCLT is described in some detail as this is a critical part of the actuator design. The assumptions are as follows: i) All layers are perfectly bonded to one another. ii) All layers are homogenous. iii) Individual layer properties can be isotropic, orthotropic, or transversely isotropic. iv) The thickness of the laminate is small compared to its length and width, resulting in a state of plane stress. v) Deformations are sufficiently small to permit the establishment of kinematics and equilibrium conditions with respect to the unperturbed neutral surface. vi) Plane sections remain plane. vii) Normals to the mid-plane have a constant length and remain normal.

The total strain in the length and width direction, ε, is broken down into the sum of the strain at the mid-plane, ε^o, due to the average axial load in the laminate, and the strains associated with curvature, κ, due to the average bending moment in the laminate.

$$\{\varepsilon\} = \{\varepsilon^o\} + z\{\kappa\} \tag{1}$$

Here z is the location along the X_3 axis, which is through the thickness of the laminate. Note that the curvature is equal to the inverse of the radius of curvature, ρ.

The total strain is the superposition of the mechanical strain, ε^σ, the thermal strain, ε^T, and the piezoelectric strain, ε^P.

$$\{\varepsilon\} = \{\varepsilon^\sigma\} + \{\varepsilon^T\} + \{\varepsilon^P\} \tag{2}$$

The total strain from Equation (1) is substituted into Equation (2), and the mechanical, thermal, and piezoelectric strains are expanded in Equation (3). The mechanical strain is the product of compliance, s, and stress, σ, as defined by Hooke's law. The thermal strain is the product of the coefficients of thermal expansion, $\overline{\alpha}$, and the difference

between the cure temperature and room temperature, ΔT. The piezoelectric strain is the product of the piezoelectric strain coefficients, d, and the electric field, E.

$$\{\varepsilon^{\circ}\} + z\{\kappa\} = [s]\{\sigma\} + \Delta T\{\bar{\alpha}\} + \mathrm{E}\{d\} \tag{3}$$

Equation (3) can be rearranged to solve for the stress in each layer. According to Equation (4), stresses can be calculated for any z location through the thickness of the laminate. The subscript k denotes that the transformed reduced stiffness coefficients for the material in the k^{th} layer of the laminate. The transformed reduced stiffness coefficients, $\bar{Q}$, are used for the plane stress condition.

$$\{\sigma\} = [\bar{Q}]_k \left(\{\varepsilon^{\circ}\} + z\{\kappa\} - \Delta T\{\bar{\alpha}\} - \mathrm{E}\{d\}\right) \tag{4}$$

Forces and moments that act on the actuator are due to mechanical loads, differential thermal expansion, and piezoelectric coupling. For this model, the applied mechanical loads are taken to be zero. Force per unit length, N^{T}, due to thermal expansion is found by summing the stress induced by thermal expansion over each ply of the laminate, as in Equation (5). Moments per unit length, M^{T}, due to thermal expansion are also given in Equation (5).

$$\begin{aligned} \{N^{\mathrm{T}}\} &= \Delta T \sum_{k=1}^{n} [\bar{Q}]_k \{\bar{\alpha}\}_k (z_k - z_{k-1}) \\ \{M^{\mathrm{T}}\} &= \frac{1}{2} \Delta T \sum_{k=1}^{n} [\bar{Q}]_k \{\bar{\alpha}\}_k \left(z_k^2 - z_{k-1}^2\right) \end{aligned} \tag{5}$$

The strain due to piezoelectric coupling can be estimated using the linear piezoelectric constitutive law, which is given by Equation (6).

$$
\begin{aligned}
\varepsilon_{ij} &= s^{\mathrm{E}}_{ijkl}\sigma_{kl} + d_{mij}\mathrm{E}_m \\
D_k &= d_{klm}\sigma_{lm} + K^{\sigma}_{kp}\mathrm{E}_p \\
\sigma_{ij} &= c^{\mathrm{E}}_{ijkl}\varepsilon_{kl} - e_{mij}\mathrm{E}_m \\
D_m &= e_{mkl}\varepsilon_{kl} + K^{\varepsilon}_{kp}\mathrm{E}_p
\end{aligned}
\tag{6}
$$

In the above, D is electric displacement, c is elastic stiffness, e is the piezoelectric stress constant, and K is the dielectric permittivity constant.

Forces and moments due to piezoelectric coupling are given by Equation (7).

$$
\begin{aligned}
\{N^{\mathrm{P}}\} &= \mathrm{E}_3 \sum_{k=1}^{n} [\overline{Q}]_k \{d\}_k (z_k - z_{k-1}) \\
\{M^{\mathrm{P}}\} &= \frac{1}{2}\mathrm{E}_3 \sum_{k=1}^{n} [\overline{Q}]_k \{d\}_k (z_k^2 - z_{k-1}^2)
\end{aligned}
\tag{7}
$$

The forces and moments due to differential thermal expansion and piezoelectric coupling will generate mid-plane strains and curvatures according to the relationship in Equation (8).

$$
\begin{Bmatrix} N^{\sigma} + N^{T} + N^{P} \\ M^{\sigma} + M^{T} + M^{P} \end{Bmatrix} = \begin{bmatrix} A & B \\ B & D \end{bmatrix} \begin{Bmatrix} \varepsilon^{o} \\ \kappa \end{Bmatrix}
\tag{8}
$$

In Equation (8), A, B, and D are the in-plane axial stiffness matrix, the coupling stiffness matrix, and bending stiffness matrix, respectively, and are given by Equation (9). The quantities N, M, A, B, and D are known, and ε^{o} and κ are unknowns. The mechanical forces and moments, N^{σ} and M^{σ}, are zero when no boundary tractions are applied.

$$[A] = \sum_{k=1}^{N} [\bar{Q}]_k (z_k - z_{k-1})$$
$$[B] = \frac{1}{2} \sum_{k=1}^{N} [\bar{Q}]_k (z_k^2 - z_{k-1}^2) \quad (9)$$
$$[D] = \frac{1}{3} \sum_{k=1}^{N} [\bar{Q}]_k (z_k^3 - z_{k-1}^3)$$

When a curved actuator is resting on a flat plate, the distance from the plate to the center of the actuator is referred to as the dome height. Using geometry, the dome height, h, can be calculated as a function of the radius of curvature and the arc length, L, as shown in Equation (10).

$$h = \rho \left[1 - \cos\left(\frac{L}{2\rho} \right) \right] \quad (10)$$

MCLT was used to model the linear elastic response of composite actuators with multiple laminated plies that are subjected to in-plane loads and bending moments. The model was used to predict the stresses and strains through the thickness of the specimens, as well as the radius of curvature and dome height. The actuators were designed so that the piezoelectric plate was in a state of residual compression. Since the piezoelectric plates are brittle, being in residual compression renders the actuators resistant to cracking. The curvature was primarily dependent on two mechanisms, thermal expansion and piezoelectric expansion. The initial curvature of the actuator is due to thermal expansion, and the change in curvature under an applied electric field is due to piezoelectric expansion.

The following MATLAB code was used for the design of piezoelectric composite actuators:

MODIFIED CLASSICAL LAMINATION THEORY MODEL

```
%Author: Kyle G. Webber

%Purpose: To find the stresses, strains, and dome
%         height in a composite structure of an arbitrary
%         lay-up, with or without an embedded piezoelectric
%         material.

clear

A=0; B=0; D=0; nt=0; mt=0; nn=0; m=0; ne=[0;0;0];
me=[0;0;0]; r=0; j=0; g=0; k=0; posx=0; negx=0; posy=0;
negy=0; a=0; b=0; c=0; d=0;

n = input('How many layers is the composite? ');
Lx = input('What is the length of the laminate (mm)? ');
E = input('What is the applied electric field (V/m)? ');
temp = input('What is the temperature change (Celsius)? ');
num = input('From the bottom of the lay-up, which number
ply is the PZT (If no PZT, enter 0)? ');

input('The following inputs are from the bottom ply to the
top ply. Please press enter.')

z(1) = 0;

 for i = 1:n;
     fprintf('\n')
     fprintf('Input material properties for layer %d\n',i);
     E0(i) = input('What is E11 of this ply (Pa)? ');
     E90(i) = input('What is E22 of this ply (Pa)? ');
     G12(i) = input('What is the shear modulus of this
        ply (Pa)? ');
     Nu12(i) = input('What is v12 of this ply? ');
     Nu21(i) = Nu12(i)*(E90(i)/E0(i));
     alpha1(i) = input('What is the thermal expansion
        parallel to the fibers (1/C)?');
     alpha2(i) = input('What is the thermal expansion
        perpendicular to the fibers (1/C)? ');
     Theta(i) = input('What is the angle of this ply; if
        PZT layer enter 0 (radians)?  ');
     t(i) = input('How thick is the ply (mm)? ');
```

```
      z(i+1)=z(i) + (t(i)/1000);
  end

for i = 1:n;

h(1)=-(z(n+1)/2);
h(i+1)=z(i+1)-(z(n+1)/2);

%defining material properties for CTS 3195HD PZT
   d31=-190e-12;
   d32=d31;
   d33=390e-12;

%transforming the thermal expansions
alphax(i) = alpha1(i)*((cos(Theta(i)))^2) + alpha2(i)
   *((sin(Theta(i)))^2);

alphay(i) = alpha2(i)*((cos(Theta(i)))^2) + alpha1(i)
   *((sin(Theta(i)))^2);

alphaxy(i) = (2*cos(Theta(i))*sin(Theta(i)))*(alpha1(i)-
   alpha2(i));

%solving for the stiffness coefficients
Q11(i) = E0(i)/(1-(Nu12(i)*Nu21(i)));
Q22(i) = E90(i)/(1-(Nu12(i)*Nu21(i)));
Q12(i) = (Nu12(i)*E90(i))/(1-(Nu12(i)*Nu21(i)));
Q66(i) = G12(i);

%solving for the transformed reduced stiffness matrix
Q11bar(i) = Q11(i)*(cos(Theta(i))^4))+(2*(Q12(i)+
   (2*Q66(i)))*((sin(Theta(i)))^2)*((cos(Theta(i)))^2))
   +(Q22(i) *(sin(Theta(i)))^4);

Q12bar(i) = ((Q11(i)+Q22(i)-4*Q66(i))*((sin(Theta(i)))^2)*
   ((cos(Theta(i)))^2))+(Q12(i)*(((sin(Theta(i)))^4)+
   ((cos(Theta(i)))^4)));

Q22bar(i)=(Q11(i)*(sin(Theta(i))^4))+(2*(Q12(i)+(2*Q66(i)))
   *((sin(Theta(i)))^2)*((cos(Theta(i)))^2))+(Q22(i)*
   (cos(Theta(i)))^4);

Q16bar(i) = ((Q11(i)-Q12(i)-2*Q66(i))*sin(Theta(i))*
   ((cos(Theta(i)))^3))+((Q12(i)-Q22(i)+2*Q66(i))*
   cos(Theta(i)) *((sin(Theta(i)))^3));
```

```
Q26bar(i) = ((Q11(i)-Q12(i)-2*Q66(i))*cos(Theta(i))*
   ((sin(Theta(i)))^3))+((Q12(i)-Q22(i)+2*Q66(i))*
   sin(Theta(i))*((cos(Theta(i)))^3));

Q66bar(i) = ((Q11(i)+Q22(i)-2*Q12(i)-2*Q66(i))*
   ((sin(Theta(i)))^2)*((cos(Theta(i)))^2))+
   (Q66(i)*(((sin(Theta(i)))^4)+((cos(Theta(i)))^4)));

Qbar = [Q11bar(i) Q12bar(i) Q16bar(i); Q12bar(i) Q22bar(i)
   Q26bar(i); Q16bar(i) Q26bar(i) Q66bar(i)];

%normal forces due to electric field
if i == num
   ne = (Qbar)*[d31;d31;0]*(h(num+1)-h(num))*E;
end

%normal force due to thermal change
nt = nt + (((Qbar)*[alphax(i);alphay(i);alphaxy(i)])
   *temp*(h(i+1)-h(i)));

%Neglecting external forces

%moment force due to electric field
if i == num
   me = 0.5*(Qbar)*[d31;d31;0]*(((h(num+1))^2)-
        ((h(num))^2))*E;
end

%moment due to thermal change
mt = mt + ((0.5*(Qbar)*[alphax(i);alphay(i);alphaxy(i)])
   *(((h(i+1))^2)-((h(i))^2))*temp);

%Neglecting external moments

%Calculating laminate stiffnesses
A = A + (Qbar*((h(i+1)-h(i))));
B = B + ((1/2)*(Qbar)*(((h(i+1))^2)-((h(i))^2)));
D = D + ((1/3)*(Qbar)*(((h(i+1))^3)-((h(i))^3)));

end


F = [A B
     B D];

H = inv(F);
```

```
nn = ne+nt;
m = me+mt;

    NM = [nn;m];
    ek = H*NM;
    eox = ek(1);
    eoy = ek(2);
    eoxy = ek(3);
    kx = ek(4);
    ky = ek(5);
    kxy = ek(6);

    rhox = 1/ek(4);
    rhoy = 1/ek(5);

hx = rhox*1000*(1-cos(Lx/(2000*rhox)));

disp('The dome height of the actuator as determined by CLT
is [mm]') ;disp(abs(hx))

%plotting the strains over the thickness
   for q = h(1)*1000:.01:-h(1)*1000
           g = g+1;
           r(g) = q/1000;
           ex(g) = (r(g)/rhox+eox)*1e6;
           ey(g) = (r(g)/rhoy+eoy)*1e6;
   end


%Plot of strains in x-direction
   figure
   plot(ex,r*1000,'r')
   hold on

   for i = 1:n;
           plot([ex(1) ex(g)],[h(i) h(i)]*1000)
   end

    plot([ex(1) ex(g)],[h(n+1) h(n+1)]*1000)
    xlabel('Epsilon_x_x (um/m)')
    ylabel('Thickness (mm)')


%Plot of strains in y-direction
   figure
   plot(ey,r*1000,'g')
   hold on
```

```
    for i = 1:n;
            plot([ey(1) ey(g)],[h(i) h(i)]*1000)
    end

     plot([ey(1) ey(g)],[h(n+1) h(n+1)]*1000)
     xlabel('Epsilon_y_y (um/m)')
     ylabel('Thickness (mm)')


resolution = 0.001;

%Plotting the stresses over the thickness
for i = 1:n
   for v = h(i+1)*1000:-resolution:h(i)*1000
       k = k+1;
       j(k) = v/1000;

       if i == num
          sigmax(k)=([Q11bar(i) Q12bar(i) Q16bar(i)]*
          [eox;eoy;eoxy]+[Q11bar(i) Q12bar(i) Q16bar(i)]*
          j(k)*[kx;ky;kxy]-[Q11bar(i) Q12bar(i) Q16bar(i)]
          *[alphax(i);alphay(i);alphaxy(i)]*temp-[Q11bar(i)
          Q12bar(i) Q16bar(i)]*[d31;d31;0]*E)/1e6;

          sigmay(k)=([Q12bar(i) Q22bar(i) Q26bar(i)]*
          [eox;eoy;eoxy]+[Q12bar(i) Q22bar(i) Q26bar(i)]
          *j(k)*[kx;ky;kxy]-[Q12bar(i) Q22bar(i) Q26bar(i)]
          *[alphax(i);alphay(i);alphaxy(i)]*temp-[Q12bar(i)
          Q22bar(i) Q26bar(i)]*[d31;d31;0]*E)/1e6;

       else
          sigmax(k)=(([Q11bar(i) Q12bar(i) Q16bar(i)]*
          [eox;eoy;eoxy])+([Q11bar(i) Q12bar(i) Q16bar(i)]
          *j(k)*[kx;ky;kxy])-([Q11bar(i) Q12bar(i)
          Q16bar(i)] *[alphax(i);alphay(i);alphaxy(i)]*
          temp))/1e6;

          sigmay(k)=(([Q12bar(i) Q22bar(i) Q26bar(i)]*
          [eox;eoy;eoxy])+([Q12bar(i) Q22bar(i) Q26bar(i)]
          *j(k)*[kx;ky;kxy])-([Q12bar(i) Q22bar(i)
          Q26bar(i)]*[alphax(i);alphay(i);alphaxy(i)]*
          temp))/1e6;
       end

%Checking the equilibrium.
```

```
 if k > 1
   if sigmax(k)>0
    posx = posx + (((sigmax(k)+sigmax(k-1))/2)*resolution);
   else
    negx = negx + (((sigmax(k)+sigmax(k-1))/2)*resolution);
   end

   if sigmax(k)>0
    posy = posy + (((sigmay(k)+sigmay(k-1))/2)*resolution);
   else
    negy = negy + (((sigmay(k)+sigmay(k-1))/2)*resolution);
   end
 end
end
end

  if abs(posx + negx) < 0.1
   disp('Laminate is in equilibrium in x-direction')
  else
   disp('Laminate is not in equilibrium in x-direction')
  end

  if abs(posy + negy) < 0.1
   disp('Laminate is in equilibrium in y-direction')
  else
   disp('Laminate is not in equilibrium in y-direction')
  end

%Plot of stresses in x-direction
figure
plot(sigmax,j*1000,'r.')
hold on

for i = 1:n;
 plot([min(sigmax) max(sigmax)],[h(i) h(i)]*1000)
end

plot([min(sigmax) max(sigmax)],[h(n+1) h(n+1)]*1000)
 xlabel('Sigma_x_x (MPa)')
 ylabel('Thickness (mm)')


%Plot of stresses in y-direction
figure
plot(sigmay,j*1000,'g.')
hold on
```

```
for i = 1:n;
 plot([min(sigmay) max(sigmay)],[h(i) h(i)]*1000)
end

plot([min(sigmay) max(sigmay)],[h(n+1) h(n+1)]*1000)
 xlabel('Sigma_y_y (MPa)')
 ylabel('Thickness (mm)')
```